Contribution from the Department of Chemistry, University of Western Ontario, London, Ontario, Canada, and Chemistry Division, National Research Council of Canada, Ottawa, Canada

High-Resolution He I and He II Photoelectron Spectra of $TiCl_4$, $SnCl_4$, and $(CH_3)_4Sn$

G. M. BANCROFT,*[1] E. PELLACH,[1] and J. S. TSE[1,2]

Received March 4, 1982

High-resolution He I and He II photoelectron spectra of $TiCl_4$, $SnCl_4$, and $(CH_3)_4Sn$ have been reported. A number of new peaks have been resolved in these spectra which have led to a reassessment of previous $TiCl_4$ assignments. We suggest that the ordering of the three high binding valence levels in $TiCl_4$ should be $(1e \sim 2a_1) < 3t_2$ rather than $(1e_1, 3t_2) < 2a_1$, as proposed earlier. This order is consistent with theoretical SCF–Xα predictions, cross-section and vibrational calculations, and intensity changes in the He I and He II spectra of $SnCl_4$ and $(CH_3)_4Sn$.

Introduction

Ultraviolet photoelectron spectroscopy (UPS) has proven to be of central importance in elucidating the molecular orbital sequences in a wide range of inorganic molecules (for example, see the recent review on transition metal compounds[3]). In many cases, however, the valence-band spectra are very complex, and the assignments are difficult to make. In the last few years, molecular orbital calculations combined with theoretical cross-section changes between He Iα (21.2 eV) and He IIα (40.8 eV) spectra[4–8] have aided the assignments.

Despite the availability of high-quality molecular orbital calculations and He I and He II spectra, the assignment of many spectra in the literature is controversial. A good example of the assignment problems is provided by the UPS spectra of the relatively simple but fundamentally important molecule $TiCl_4$. Experimental He I spectra have been published five times,[5,9–12] the He II spectrum has been reported,[5] and a large number of molecular orbital calculations have been published, including INDO,[13] SCF–Xα,[11,14,15] and ab initio[16] calculations. Despite all of this effort, Cowley states[3] that some of "the bands in the $TiCl_4$ spectrum cannot be assigned unequivocably" because the calculations differ in the sequencing of molecular orbitals and the UPS bands are quite closely spaced.

All of the above $TiCl_4$ spectra, and most of the spectra of inorganic molecules in the literature, have been recorded at medium resolutions, usually about 60 meV for He I spectra and 100 meV for He II spectra. In our studies of ligand field splittings and valence-band spectra, we have observed resolutions for *both* He I and He II spectra in the 30–50-meV region.[7,17,18] In this paper, we use this high-resolution combined with theoretical cross-section and vibronic coupling calculations to show up several additional features in the $TiCl_4$ spectra which lead to a reassessment of the spectral assignments. We also report selected spectra of $SnCl_4$ and $(CH_3)_4Sn$ to enable us to understand better the intensity changes between He I and He II $TiCl_4$ valence-band spectra.

Experimental Section

(A) Ultraviolet Photoelectron Spectra. High-purity $TiCl_4$ and $SnCl_4$ were purchased from Fisher Scientific. $SnCl_4$ was distilled prior to recording its photoelectron spectra. $(CH_3)_4Sn$ was prepared according to the method described by Edgell and Ward.[19] The purity of this compound was confirmed by NMR.

All photoelectron spectra were measured in a McPherson ESCA 36 spectrometer at room temperature with use of a hollow cathode lamp described previously.[17] The spectra were obtained by multiscanning the region of interest. We routinely obtain Ar $3p_{3/2}$ line widths of 17 and 26 meV with He I and He II radiation, respectively. $TiCl_4$ proved to be a very difficult compound to work with. After spectra were run for a short time, it destroyed our channeltron detectors. The statistics on our He II spectrum are not as good as those on our normal He II spectra because of this problem.

The photoelectron peaks were fitted with a Voigt function simulated by a linear combination of Gaussian–Lorentzian line shapes.[20] Four parameters are used to describe each photoelectron peak: the peak position (binding energy), the full width at half-maximum (fwhm), the peak height (YMAX), and the Gauss fraction (GFAC), which is a measure of the Gaussian character of the peak. The "goodness of fit" criterion requires that the sum of the squares of the deviation from the best fit divided by the variance of a single count is minimized. From the fitting procedure, we obtain the best estimates (and standard deviations) for the four peak parameters.

(B) Theoretical Calculations. To confirm the proposed assignments for $TiCl_4$ and $SnCl_4$, we have performed theoretical photoionization cross-section calculations for all the valence molecular orbitals as a function of the photon energy using the Xα–SW method.[21,22] In this method, the continuum wave functions for the photoelectrons are generated from the ground-state Xα–SW molecular potential. Therefore, the continuum orbitals possess the correct molecular symmetry and orthogonality to the ground-state wave functions.[23] All symmetry-allowed photoionization processes (dipolar selection rule) are included in the calculation. From previous experience,[24,25] we learned that for big molecules, the absolute magnitude of the theoretical photoionization cross section is very sensitive to the completeness of the partial wave expansion of the continuum wave functions. The merit of the Xα–SW method in predicting photoionization cross sections for molecules has been established in several recent studies.[24–27]

(1) University of Western Ontario.
(2) National Research Council of Canada.
(3) Cowley, A. H. *Prog. Inorg. Chem.* **1979**, *26*, 45.
(4) Higginson, B. R.; Lloyd, D.; Evans, S.; Orchard, A. R. *J. Chem. Soc., Faraday Trans. 2* **1975**, *71*, 1913.
(5) Egdell, R. G.; Orchard, A. F.; Lloyd, D. R.; Richardson, N. V. *J. Electron. Spectrosc. Relat. Phenom.* **1977**, *12*, 415.
(6) Egdell, R. G.; Fragala, I. L.; Orchard, A. F. *J. Electron Spectrosc. Relat. Phenom.* **1979**, *17*, 267.
(7) Creber, D. K.; Bancroft, G. M. *Inorg. Chem.* **1980**, *19*, 645 and references therein.
(8) Van-Dam, H.; Oskam, A. *J. Electron. Spectrosc. Relat. Phenom.* **1979**, *16*, 307.
(9) Cox, P. A.; Evans, S.; Hammett, A.; Orchard, A. F. *Chem. Phys. Lett.* **1970**, *7*, 414.
(10) Green, J. C.; Green, M. L. H.; Joachim, P. J.; Orchard, A. F.; Turner, D. W. *Philos. Trans. R. Soc. London, Ser. A* **1970**, *268*, 111.
(11) Burroughs, P.; Evans, S.; Hamnett, A.; Orchard, A. F.; Richardson, N. V. *J. Chem. Soc., Faraday Trans. 2* **1974**, *70*, 1895.
(12) Egdell, R. G.; Orchard, A. F. *J. Chem. Soc., Faraday Trans. 2* **1978**, *74*, 485.
(13) Truax, D. R.; Greer, J. A.; Ziegler, T. *J. Chem. Phys.* **1973**, *59*, 6662.
(14) Parameswaron, T.; Ellis, D. E. *J. Chem. Phys.* **1973**, *58*, 2088.
(15) Tossell, J. A. *Chem. Phys. Lett.* **1979**, *65*, 371.
(16) Hillier, I. H.; Kendrick, J. *Inorg. Chem.* **1976**, *15*, 520.
(17) Coatsworth, L. L.; Bancroft, G. M.; Creber, D. K.; Lazier, R. J.; Jacobs, P. W. M. *J. Electron. Spectrosc. Relat. Phenom.* **1978**, *13*, 395.
(18) Bancroft, G. M.; Coatsworth, L. L.; Creber, D. K.; Tse, J. S. *Phys. Scr.* **1977**, *16*, 217.
(19) Egdell, W. F.; Ward, C. W. *J. Chem. Soc.* **1954**, 1169.
(20) Bancroft, G. M.; Idams, I.; Coatsworth, L. L.; Bennewitz, C. D.; Brown, J. D.; Westwood, W. D. *Anal. Chem.* **1975**, *47*, 586.
(21) Dill, D.; Dehmer, J. L. *J. Chem. Phys.* **1974**, *61*, 692.
(22) Davenport, J. W. *Phys. Rev. Lett.* **1976**, 945.
(23) Siegel, J.; Dill, D.; Dehmer, J. L. *J. Chem. Phys.* **1976**, *64*, 3204.
(24) Roche, M.; Salahub, D. R.; Messmer, R. P. *J. Electron. Spectrosc. Relat. Phenom.* **1980**, *19*, 273.
(25) Grimm, F. A.; Carlson, T. A.; Dress, W. B.; Agram, P.; Thomson, J. O.; Davenport, J. W. *J. Chem. Phys.* **1978**, *72*, 3041.
(26) Levinson, H. J.; Gustafsson, T.; Soven, P. *Phys. Rev. A* **1979**, *19*, 1089.
(27) Gustafsson, T.; Levinson, H. J. *Chem. Phys. Lett.* **1981**, *78*, 28.

0020-1669/82/1321-2950$01.25/0

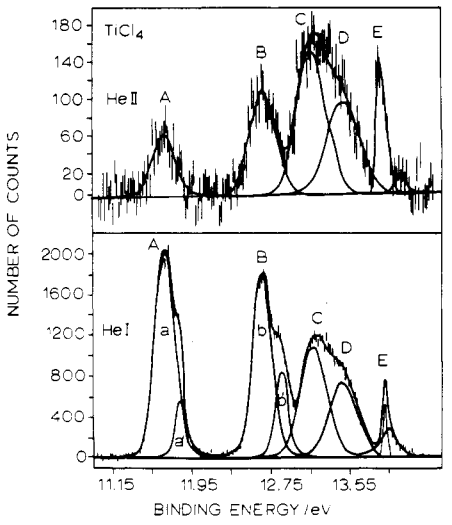

Figure 1. He I and He II photoelectron spectra of $TiCl_4$.

In order to establish the reliability of the present theoretical results, we have performed calculations with the maximum azimuthal quantum number for the continuum wave functions expanded to $l = 5$ and $l = 7$. Tangential spheres were used in all calculations.

We have obtained qualitative agreement for the variation of the photoionization cross sections with photon energy from both calculations. We observed that there are moderate variations in the absolute magnitude of the cross sections. However, this should not affect the qualitative picture below.

We adopted the Green's function method to calculate the vibrational structure for the molecular ions.[28,29] The renormalized ionization energies and vibronic coupling parameters are calculated by the diagonal 2ph–TDA (two-particle-hole Tamm–Dancoff approximation) procedure.[29] The relevant ground-state wave functions and various Coulomb and exchange integrals are obtained from an INDO/2S program parameterized for transition metal compounds.[30,31]

Results and Discussion

(A) Valence-Band Spectra and Assignment. The He I and He II photoelectron spectra of the entire $TiCl_4$ valence-band region are shown in Figure 1, while narrow energy scans of small regions of the He I spectrum are shown in Figure 2. All peak parameters for these spectra are given in Table I. The gross features of our spectra compare well with the spectra reported previously.[5,9-12]

Using Orchard's[5] band notation, we find four well-resolved bands at 11.7 eV (A), 12.8 eV (B), 13.2 eV (C + D), and 13.9 eV (E). Closer examination of our spectra in Figures 1 and 2 reveals that every one of these bands is composed of two or more peaks. The statistics in the He II spectrum are not good enough to resolve the finer details in the bands A, B, and E. Our instrumental resolution is indicated by the 30-meV line widths of the component peaks of band E (Figure 2C and Table I). None of the previously published spectra of $TiCl_4$ showed even any signs of asymmetry on this band.

In the tetrahedral $TiCl_4$ molecule, the metal–halogen bonding molecular orbitals transform as $e + t_2$ symmetries, and the halogen lone pairs, as $t_1 + t_2 + e + a_1$ symmetries. The assignment of bands A and B to the $1t_1$ and $3t_2$ orbitals, respectively, of largely Cl 3p character is generally agreed on,[3,5] and our spectra are consistent with this assignment. Both bands A and B show very distinct shoulders, and these bands have both been fitted to two peaks—a and a′ separated by 146 meV and b and b′ separated by 190 meV (Table I). These distinct shoulders, giving these large splittings, preclude the

Table I. Valence-Band Parameters of $TiCl_4$ (in eV)[a]

	Orchard et al.[5,9-12]				this work										
		rel area			He I						He II				
band	BE	He I	He II	assignt	BE[d]	ΔE	fwhm[d]	GFAC[d]	YMAX[b,d]	area[c]	fwhm	GFAC	YMAX[b]	area[c]	assignt
A	11.76	3.0	3.0	$1t_1$	11.69	0.15	0.23 (1)	0.92 (4)	2045 (41)	55.0 (2.0)	0.26	0.75 (69)	66 (9)	7.1 (2.6)	$1t_1$
					11.84		0.09 (2)	0.16 (31)	578 (89)	7.9 (2.0)	0.03				
B	12.77	3.0	4.3	$3t_2$	12.67	0.19	0.21 (1)	0.93 (4)	1804 (37)	50.0 (2.0)	0.29	1.00	110 (6)	12.2 (0.8)	$3t_2$
					12.86		0.15 (2)	1.00	836 (64)	16.4 (2.4)	(0.02)				
C	13.25	4.2	12.9	$1e + 2t_2$	13.17		0.31 (4)	1.00	1034 (123)	42.6 (9.6)	0.34[f]	1.00	150 (6)	19.7 (0.8)	$1a_1 + 1e$
D	...				13.46	0.29	0.35 (4)	1.00	784 (106)	37.9 (9.4)	(0.38)[f]	1.00	100 (7)	14.8 (1.0)	
					13.88		0.028[e]	0.75	204 (25)						
					13.91	0.035	0.032[e]	0.90	2392 (32)		0.10	1.0	136 (11)	5.7 (0.5)	
E	13.96	0.6	4.0	$2a_1$	13.95	0.035	0.032[e]	0.90	1000 (33)	11.4 (3.6)	(0.01)				$2t_2$
					13.98	0.030	0.032[e]	0.90	420 (31)		0.12	1.0	14	1.0 (0.5)	
					14.01	0.033	0.028[e]	0.75	386 (25)		(0.07)				

[a] Errors given in parentheses. [b] Number of counts. [c] Arbitrary units divided by KE for normalization. [d] The values for band E are from the fitting spectrum of Figure 2C. [e] fwhm constrained in the range of the main peak in band E. [f] fwhm constrained in the range of fwhm of He I spectrum.

(28) Cederbaum, L. S.; Domcke, W. *J. Chem. Phys.* **1974**, *60*, 2878.
(29) Cederbaum, L. S.; Domcke, W. *Adv. Chem. Phys.* **1977**, *36*, 205.
(30) Bacon, A. D.; Zerner, M. C. *Theor. Chim. Acta* **1979**, *53*, 21.
(31) Zerner, M. C.; Loew, G. H.; Kirchner, R. E.; Mueller-Westerhoff, U. T. *J. Am. Chem. Soc.* **1980**, *102*, 589.

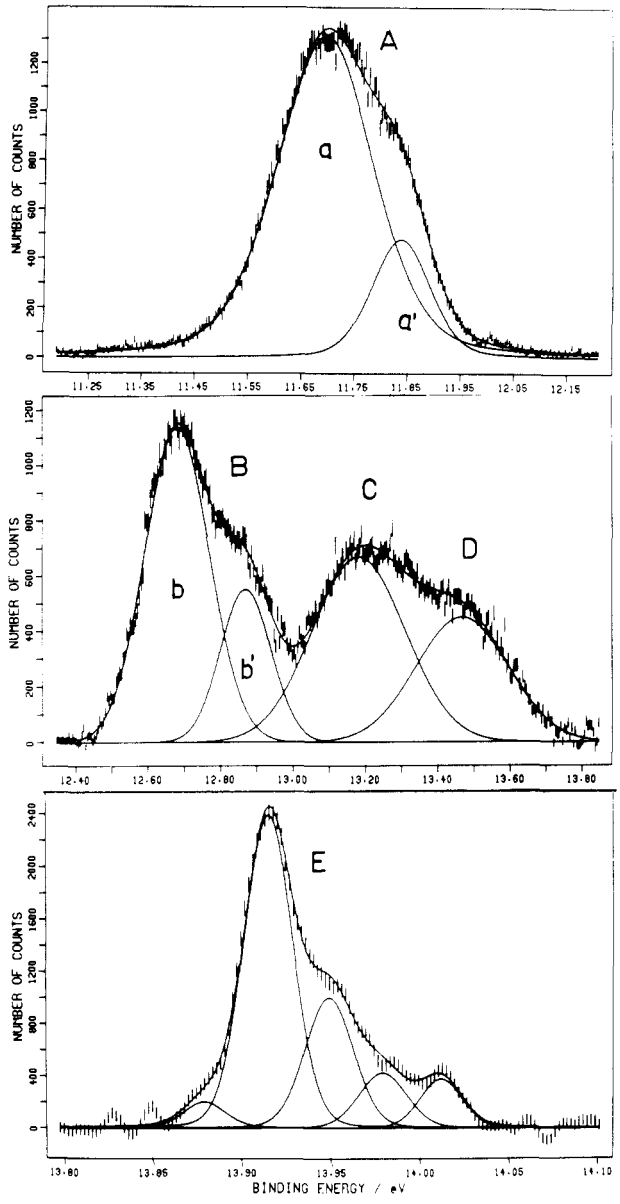

Figure 2. Expanded He I photoelectron spectra of $TiCl_4$: (A) band A; (B) bands B, C, and D; (C) band E.

two doublets being due solely to vibrational structure. Other possible causes are spin–orbit splitting and Jahn–Teller splitting.[11,12] Both Cl 3p spin–orbit splittings (≤73 meV) and Jahn–Teller splittings are normally considerably smaller than our observed splitting,[11,12,32] but both are well-known in tetrahedral AB_4 molecules.[11,12] The overall observed structure is probably due to a combination of vibrational, spin–orbit, and Jahn–Teller splittings. The vibrational broadening is calculated below.

The assignment of the next three peaks has been in dispute. Orchard et al. proposed two peaks in the C + D band region and assigned them to the 1e and $2t_2$ orbitals without specifying the order. They assigned band E to the $2a_1$ orbital.[10-12] Combined with molecular orbital calculations, our spectra strongly suggest (but do not prove unequivocally) that the order of levels is not 1e, $2t_2 < 2a_1$ but rather $(1e \sim 2a_1) < 2t_2$.

Figures 1 and 2B show that the C + D region contains two peaks separated by 0.29 eV. The four-peak structure in band E resembles a normal vibrational progression. We associate

Table II. Calculated MO Charge Distribution of $TiCl_4$ from the Xα–SW Method

		% charge distribution					
		Ti					
band	orbital	d	s	p	Cl	outsphere	intersphere
A	$1t_1$		...		81	1	17
B	$3t_2$			2	76	2	21
C	1e	12			66	1	21
D	$2a_1$		7		75	3	14
E	$2t_2$	25		1	63	2	9

the 33-meV energy difference (266 cm^{-1}) with the ν_1 fundamental $TiCl_4$ vibration of 388 cm^{-1}.[33] This substantial reduction observed in the ν_1 energy (31%) is extremely similar to that observed on the corresponding highest binding energy band in the $SiCl_4$ spectrum.[6] In both cases, this structure must arise from a bonding M–Cl molecular orbital.

The relative intensities of the He I and He II peaks are crucial in the interpretation. The intensity of bands A, B, and D diminish relative to C on going from He I to He II, while band E increases sharply. It has often been shown that the Cl 3p cross section decreases from He I to He II, while the metal d orbital cross section increases.[34] Following this empirical "rule", we would expect bands A, B, and D to be associated with mostly Cl 3p character, with bands C and E being associated with orbitals with substantial Ti 3d character.

Before assigning bands C, D, and E with the above intensity and vibrational information, it is important to examine the latest ab initio and Xα calculations. The ab initio calculation[16] assigns these last three orbitals to $1e < 2t_2 < 2a_1$, with 16%, 21%, and 9% Ti 3d character, respectively. This assignment agrees with that of Orchard et al.[5] The Xα calculations[11,15] give the order $1e < 2a_1 < 2t_2$ but do not give orbital characters. To obtain these orbital characters, we have performed an SCF–Xα–SW calculation[35] on $TiCl_4$. The relative ordering of our ionization energies calculated by the transition-state procedure[36] agrees with the results of the previous Xα calculations and our INDO calculation described below. The charge distribution from the calculation is given in Table II. The results agree qualitatively with those from the ab initio calculations, with the Ti 3d character in these three orbitals decreasing in the order $2t_2 > 1e > 2a_1$.[37,38]

The Xα assignment $(1e < 2a_1 < 2t_2)$ is also consistent with the variation of He I and He II intensities, the vibrational structure on band E, and the order of increasing Ti 3d character in these orbitals from both Xα and ab initio calculations. The two molecular orbitals with highest Ti 3d character ($2t_2$, 1e) increase in intensity the most from He I to He II, while the Cl 3p orbitals decrease the most. The orbital with the largest bonding character ($2t_2$) gives rise to the vibrational structure with a vibrational spacing ν_1 much reduced from ν_1 for the neutral molecule.

It is interesting to note that the intensity ratio between band C and D does not change significantly from He I (1.13) to He II (1.32) radiation. A possible explanation for this observation is that vibrational and Jahn–Teller structure on the 1e orbital (band C) may accidentally overlap with the $2a_1$

(32) Coulson, C. A.; Strauss, H. L. *Proc. R. Soc. London, Ser. A* **1962**, *269*, 443.
(33) (a) Griffiths, J. E. *J. Chem. Phys.* **1968**, *49*, 642. (b) Shimanouchi, T. *J. Phys. Chem. Ref. Data* **1974**, *3*, 278.
(34) Rabalais, J. W. "Principles of Ultraviolet Photoelectron Spectroscopy"; Wiley: New York, 1977.
(35) Johnson, K. H. *Adv. Quant. Chem.* **1973**, *7*, 143.
(36) Slater, J. C. *Adv. Quant. Chem.* **1972**, *6*, 1.
(37) The $2a_1$ orbital can have no metal d character by symmetry; however, in an ab initio calculation, six functions are usually used to represent the d orbitals. A linear combination of the wave functions gives an orbital of s symmetry.
(38) Evans, J.; Green, J. C.; Joachim, P. J.; Orchard, A. F.; Turner, D. W.; Maier, J. P. *J. Chem. Soc., Faraday Trans. 2* **1972**, 905.

Table III. $SnCl_4$ Valence-Band (11–13 eV) He I and He II Parameters (eV)

	He Iα				He IIα			
peak	ΔE[a]	fwhm[a]	GFAC[a]	area[b]	ΔE[a]	fwhm[a]	GFAC[a]	area[b]
A	0.0	0.34 (1)	0.93 (6)	43.4	0.0	0.32 (3)	0.69 (22)	30.4
b	0.23 (1)	0.14 (1)	1.0	15.1	0.25 (2)	0.14 (2)	1.0	20.2
b′	0.41 (1)	0.12 (1)	0.62 (21)	13.5	0.40 (2)	0.12 (2)	0.60	15.9
C	0.64 (1)	0.18 (1)	0.73 (2)	28.1	0.64 (1)	0.19 (1)	0.70	21.8

[a] Errors given in parentheses. [b] Areas given in arbitrary units.

orbital forming band D. We cannot pinpoint, then, the $2a_1$ peak in these spectra.

Other more subtle intensity changes are apparent in the $TiCl_4$ spectrum, and these are not as readily rationalized. Bands A, B, and D are almost entirely Cl 3p in character from both ab initio and Xα calculations, and yet the area ratio of A:B:D varies substantially between He I and He II spectra (Table I). Could this substantial change in ratio be due to the very small amount of Ti 4p character [2% (Table II) or 4%[16]] in the $3t_2$ orbital or Ti 4s character in the $2a_1$ orbital, which gives rise to bands B and D, respectively? To answer this question and to further confirm our assignment of the $2a_1$ and $3t_2$ orbitals in $TiCl_4$, we recorded the He I and He II spectra of the low binding energy region of $SnCl_4$ and $(CH_3)_4Sn$.

The $SnCl_4$ spectra (11–13-eV region) are shown in Figure 3 and the peak parameters are summarized in Table III. Although previous spectra did not resolve peaks b and b′,[6] our assignment of these bands is the same as that given previously for $SnCl_4$.[6,10] We assign band A to the chlorine 3p nonbonding $1t_1$ orbital, band B to the Jahn–Teller (or spin–orbit) split slightly bonding $3t_2$ orbital, and band C to the chlorine 3p nonbonding 1e orbital. This is the same orbital ordering as in $TiCl_4$, but here there is no possibility of d-orbital involvement in the $SnCl_4$ bonding. The nonbonding natures of the $1t_1$ and 1e orbitals are ensured by symmetry, while our Xα–SW calculation on $SnCl_4$ shows that as for $TiCl_4$, the $3t_2$ orbital possess a very small amount (1.6%) of metal (Sn 5p) character.

It is particularly interesting that the area ratio of C:A remains constant at ~0.7 for $SnCl_4$ for both He I and He II spectra, whereas for $TiCl_4$ this ratio changed from ~0.6 to ~2.5 from He I to He II (Table I). These ratios are consistent with the qualitative cross-section arguments given previously. The $1t_1$ and 1e orbitals in $SnCl_4$ are entirely Cl 3p in character, and we would expect the ratio C:A to remain constant. In contrast, the 1e orbital in $TiCl_4$ has some Ti 3d character (Table III) and band C increased relative to band A on going from the He I to He II spectra. This difference in the relative cross section of band C between $TiCl_4$ and $SnCl_4$ further substantiates our assignment of band E to the $2t_2$ orbital in $TiCl_4$, which has large 3d character. The large d character in the $2t_2$ orbital should result in a large increase in band E from He I to He II as is observed.

Figure 3 and Table III show that, as for $TiCl_4$, band B in $SnCl_4$ increases in intensity relative to band A from He I and He II spectra. The ratio A:B varies from 1.5 to 0.8 for the He I and He II spectra, respectively. Again a very small amount of metal p character (1.6% Sn 5p) has apparently resulted in a very noticeable relative increase in intensity from He I to He II.

To obtain a better indication of the photon energy dependence of metal valence p orbitals, we recorded both He I and He II spectra of $(CH_3)_4Sn$. Our He I spectrum is very similar to the one recorded previously[38] and consists of two very broad peaks at 9.7 eV (X) and 13.4 eV (Y). To the best of our knowledge, the He II spectrum has not been published previously. The peak at 9.7 eV has been assigned to the Sn–C $3t_2$ orbital,[38] while the 13.4-eV peak is assigned to C–H molecular orbitals. The area ratio X:Y increases sharply from

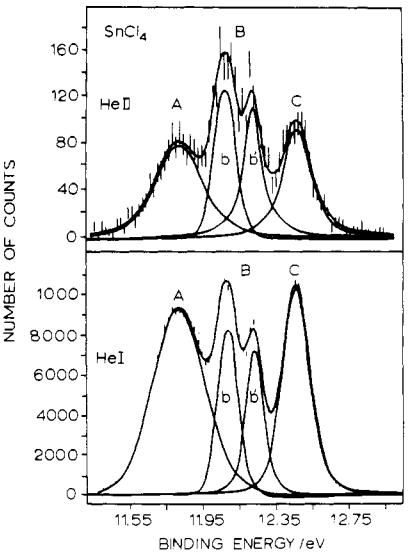

Figure 3. He I and He II photoelectron spectra of $SnCl_4$ in the 11–13-eV binding energy region.

Table IV. Photoionization Cross-Section Calculations for $TiCl_4$ and $SnCl_4$ at He I and He II Photon Energy (in Mb)

	$TiCl_4$		$SnCl_4$	
	He I	He II	He I	He II
$1t_1$	22.0	0.04	31.0	0.05
$3t_2$	41.0	0.28	29.5	1.60
1e	17.1	0.80	19.9	0.55
$2a_1$	5.36	0.015	3.5	0.17
$2t_2$	2.11	6.69	18.2	1.02

He I (0.22) to He II (0.46). It is well-known that M–C orbitals have 30–40% metal p character,[39,40] and so we expect that the Sn 5p character in the $3t_2$ orbital will also lie in this range. Since the C–H cross sections decrease by less than a factor of 2 from He I to He II,[7] the Sn 5p cross section must increase on going from He I to He II spectra.

We turn again to the A:B ratio in the tetrachlorides. It is well-known that the Cl 3p nonbonding cross section decreases much more rapidly than the C–H cross section on going from He I to He II.[5,41] A good example of this behavior is given in the spectra of $(CH_3)_3SnCl$.[41] It is also important to note the dramatic decrease in the neighboring Ar 3p cross section from He I to He II by a factor of about 10.[42] With this drastic decrease in Cl 3p cross section, and an increasing metal p cross section, a relatively small metal p character (~5%) in the $3t_2$ orbital could lead to the changes observed in the $SnCl_4$ and $TiCl_4$ A:B ratio.

(B) Photoionization Cross-Section and Vibrational Calculations. To further our understanding of photoionization

(39) Bancroft, G. M.; Creber, D. K.; Ratner, M. A.; Moskowitz, J. W.; Topiol, S. *Chem. Phys. Lett.* **1977**, *50*, 233.
(40) Bancroft, G. M.; Creber, D. E.; Basch, H. *J. Chem. Phys.* **1977**, *67*, 4891.
(41) Fragala, I.; Ciliberto, E.; Egdell, R. G.; Granozzi, G. *J. Chem. Soc., Dalton Trans.* **1977**, *55*, 3487.
(42) Samson, J. A. R. *Adv. At. Mol. Phys.* **1966**, *2*, 178.

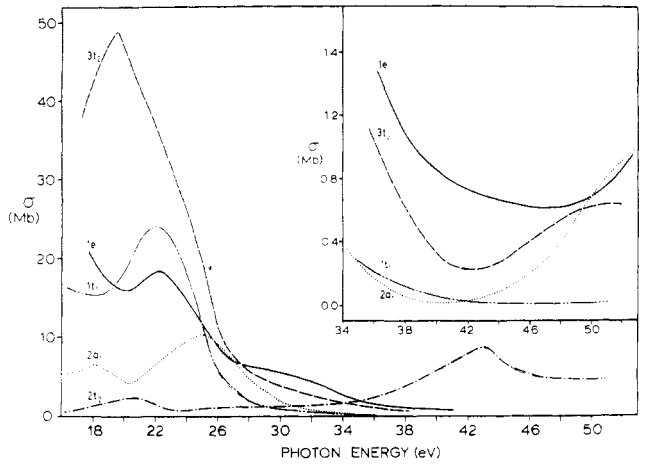

Figure 4. Calculated cross sections (Mb) for the valence molecular orbitals of $TiCl_4$ as a function of photon energy. The high photon energy region (34–52 eV) is shown in an expanded scale in the insert.

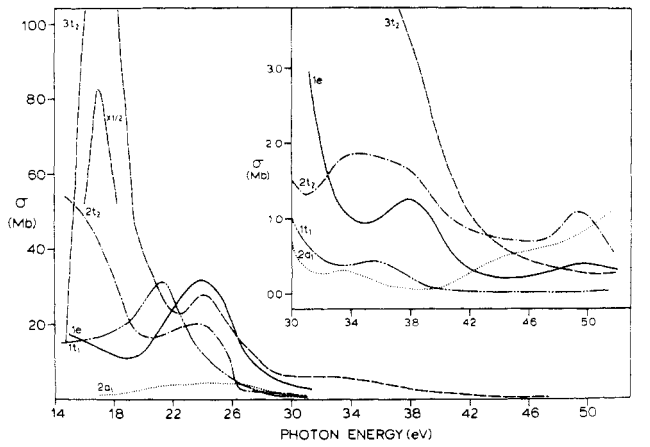

Figure 5. Calculated cross sections (Mb) for the valence molecular orbitals of $SnCl_4$ as a function of photon energy. The high photon energy region (30–52 eV) is shown in an expanded scale in the insert.

cross-section variations, we undertook the theoretical cross-section calculations on $TiCl_4$ and $SnCl_4$. The results of these calculations are summarized in Figures 4 and 5 (for $l = 7$ with an energy increment of 0.17 Ry). The specific cross sections at the He I and He II photon energies are given in Table IV.

From Tables I, III, and IV one can see that qualitatively there is good agreement between the theoretical and experimental results. In the case of $TiCl_4$, the cross section of the Cl p type orbitals ($1t_1$, $3t_2$, and $2a_1$) indeed diminish relative to 1e on going from He I to He II, while orbital $2t_2$, which has 25% d character, increases sharply. This supports our assignment for band E as the $2t_2$ orbital and not as $2a_1$.[10-12] The calculations also reflect the variation in the area ratio of A:B:D between He I and He II. It seems that a small amount of Ti 4p character in the $3t_2$ orbital enhances the cross section relative to the $1t_1$ orbital, which cannot have any metal character. If the area of band D is dominated by the vibrational and Jahn–Teller splitting of the 1e orbital as we have suggested, it is also clear from the cross-section data why band D is more intense than bands A and B in the He II spectrum.

In the case of $SnCl_4$, even though the cross-section ratio $1e:1t_1$ (C:A) changes from He I ($\sim$0.65) to He II ($\sim$11) whereas experimentally it remains almost a constant ($\sim$0.7), the calculations do show that a small amount of Sn 5p character in the $3t_2$ orbital enhance the cross section relative to the $1t_1$ and 1e orbitals, which are pure Cl p type orbitals.

Figures 4 and 5 show shape resonance effects on some of the molecular orbitals at about 10 eV above threshold, with the strongest effect on the $3t_2$ orbital. These shape resonances

Table V. Calculated Koopmans and Renormalized Ionization Energies (eV) and Renormalized Electron-Vibration Coupling Constants for $TiCl_4$

orbital	$-\epsilon_i$	ϵ^R (2ph-TDA)	a^R
$1t_1$	15.21	12.53	1.18
$3t_2$	16.14	13.41	1.72
$1a_1$	16.17	14.02	1.37
1e	16.57	14.02	3.21
$2t_2$	16.94	14.84	2.54

are the result of the interaction between the photoelectron and the molecular field in the final state. This kind of "final-state effect" has been reported in diatomic molecules such as N_2[22] and NO,[27] and in polyatomic molecules such as SF_6.[26] Elaboration of these cross-section results and others on other tetrahalides will be the subject of an ensuing publication.[43] Obviously, experimental verification of these dramatic cross-section changes using synchrotron radiation should provide unambiguous assignments in these and other molecules.

To investigate the electron-vibration coupling effect in the molecular ionization spectra and to further confirm our assignments, we have computed the vibrational spectra for the valence orbitals of $TiCl_4$. Employing the new INDO/2S parameterization for transition metals,[30,31] we obtained the same ground-state valence molecular orbital sequence as predicted by Xα–SW calculations.[15] Including many body effects (electronic relaxation and correlation effects) through the diagonal 2ph–TDA procedure did not alter the orbital ordering but improved the numerical agreement of the ionization potentials with experiment considerably (Table V).

Within the adiabatic approximation,[44] the Green's function method[28,29] can be extended to include vibrational effects using only data for the ground state. It can be shown[29] that nondegenerate electronic states can only couple to totally symmetric vibrational modes in the first-order approximation. The adiabatic approximation may not be valid for degenerate electron states unless the energy difference between electron states is large compared to the vibration spacing (weak Jahn–Teller effect), and this may well not be true in our case discussed above.

There is only one totally symmetric vibrational mode for tetrahedral molecules. If we further assume no frequency change occurs due to the ionization process, the vibrational intensities follows a Poisson distribution

$$I_i(\epsilon) = \exp(-a^R{}_i)\sum_n \frac{(a^R)^n}{n!}\delta(\epsilon - \epsilon^R{}_i + n\omega) \qquad (1)$$

where $a^R{}_i$ is the coupling parameter for the ith orbital. ϵ_i is the renormalized ionization energy and $n\omega$ is the vibrational spacing. The coupling parameter can be calculated from

$$a^R{}_i = \left(\frac{k_i}{\omega}\right)^2 \qquad k_i = -\frac{1}{2^{1/2}}\frac{\partial \epsilon^R{}_i}{\partial Q}\bigg|_{Q_0}$$

where Q is the normal coordinate belonging to the A_1 symmetry representation.

Vibration-coupling constants from INDO/2S calculations for $TiCl_4$ are tabulated in Table V. The ground-state totally symmetric vibration of 388 cm^{-1} was used throughout.[33] To mimic the limited instrumental resolution of the photoelectron spectra, we have convoluted each theoretical peak with a Lorentzian function of width 0.05 eV. The theoretical vibrational spectrum of $TiCl_4$ is depicted in Figure 6. The

(43) Pellach, E.; Tse, J. S.; Davenport, J. W., to be submitted for publication.
(44) Longuet-Higgins, H. C.; Opik, U.; Pryce, M. H. L.; Sack, R. A. *Proc. R. Soc. London, Ser. A* **1958**, *244*, 1.

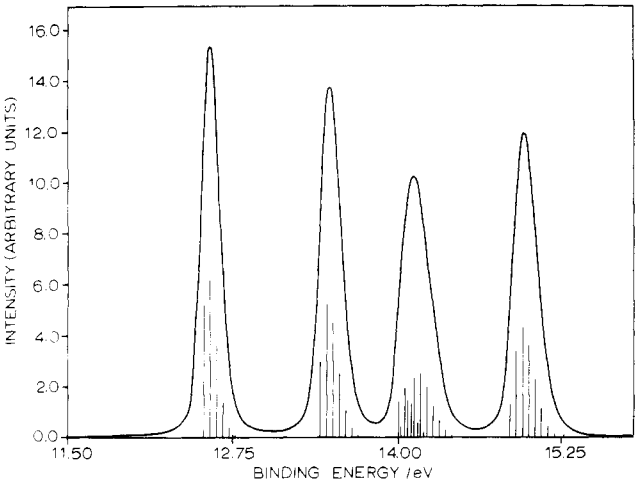

Figure 6. Theoretical vibrational spectrum of $TiCl_4$. The intensity of each peak has been weighted according to the orbital degeneracy.

magnitude of the coupling constant indicates strong vibronic coupling accompanying photoionization for all valence molecular orbitals. The relative line widths of the first three bands are qualitatively produced by the calculations. Thus the calculated full widths at half-height for the three bands A, B, (C + D) are 0.18, 0.21, and 0.30 eV. The vibrational coupling constant for the 1e orbital is the largest, and the resulting broad line partially explains the large line width for C + D. The shoulders are of course not reproduced because of the neglect of Jahn–Teller and spin–orbit splitting. Taken together with all the other experimental and theoretical evidence in this paper, our assignments must be considered relatively reliable.

Conclusions

For the relatively simple inorganic molecule $TiCl_4$, we have obtained high-resolution He I and He II spectra. In combination with $X\alpha$, INDO, cross-section, and vibrational calculations, we have shown that the previous assignment is not correct. All our evidence points to the assignment $1t_1 < 3t_2 < (1e, 2a_1) < 2t_2$. However, even with this large amount of experimental and theoretical evidence, we obviously still do not completely understand aspects of the spectrum—the shoulders on bands A, B, and C and the exact position of the $2a_1$ orbital. Valence-band spectra taken with synchrotron radiation along with more elaborate calculations are required to complete the assignments, even on this simple molecule.

Acknowledgment. We wish to thank the generosity of Professor Zerner and Dr. Davenport in furnishing the computer programs used in the present work. The financial support of the NSERC (Canada) is gratefully acknowledged. E.P. wishes to thank Bar Ilan University (Ramat-Gan, Israel) for financial support.

Contribution from the Department of Chemistry, Seton Hall University, South Orange, New Jersey 07079

Studies of the Pfeiffer Effect Developed in Tris(pyridine-2,6-dicarboxylato)terbate(III) by Phenylalkylamines, Phenylalkylamino Alcohols, and Phenylalkylamino Acids

HARRY G. BRITTAIN[1]

Received November 10, 1981

Optical activity induced in the title complex through outer-sphere complexation with a series of structurally related environment substances has been studied by means of circularly polarized luminescence (CPL) spectroscopy. The substrates were found to fall into four classes, which were determined by trends in the induced optical activity and by the nature of the functional groups on the substrates. For certain of the chiral materials, the observed optical activity was pH independent, but for others, the CPL spectra were found to invert upon ionization of the protonated ammonium group. Systematic variation of functionality on the chiral substrates enables one to conclude that ionic, hydrophobic, and hydrogen-bonding mechanisms can all contribute to the association of complex and environment substance.

Introduction

The development of optical activity in a racemic mixture of a labile metal complex upon addition of certain chiral compounds (termed the environment substance) is known as the Pfeiffer effect[2,3] and is usually thought to arise from a displacement of the equilibrium existing between the enantiomers of the racemic metal complex. While several theories have been advanced to account for the effect,[4] most of the reported work has been explained by the existence of complexation between the racemic complex and the environment substance as leading to the observed optical activity. Several attempts have been made to use the Pfeiffer effect as a means to predict absolute configurations of a variety of substances,[5-7] but these correlations have been very limited in their scope.

We have recently been using Pfeiffer optical activity to study f–f optical activity in trigonal lanthanide complexes, since these complexes are too labile to be resolved by ordinary physical or chemical means. Our work has centered on the tris lanthanide complexes of pyridine-2,6-dicarboxylic acid (DPA, or dipicolinic acid), as this ligand is known to form very strong complexes with all members of the lanthanide series[8] and the tris complex is known to possess an approximate D_3 symmetry in fluid solution at room temperature.[9] The first studies were involved with determinations of conditions under which the effect could be observed, and it was found that the $Tb(DPA)_3^{3-}$ complex could associate with chiral environment substances through both ionic (resolved tris(ethylenediamine)chromium(III)[10]) and hydrophobic (L-ascorbic acid[11]) mechanisms.

The studies involving hydrogen bonding of environment substances to aromatic portions of the DPA ligands were found to be of extreme interest, and we have recently studied the pH

(1) Teacher-Scholar of the Camille and Henry Dreyfus Foundation, 1980–1985.
(2) Kirschner, S. *Rec. Chem. Prog.* **1971**, *32*, 39.
(3) Kirschner, S.; Ahmad, N.; Munir, C.; Pollock, R. J. *Pure Appl. Chem.* **1979**, *51*, 913.
(4) Schipper, P. E. *Inorg. Chim. Acta* **1975**, *12*, 199.
(5) Miyoshi, K.; Matsumoto, Y.; Yoneda, H. *Inorg. Chem.* **1981**, *20*, 1057.
(6) Kane-Maguire, N. A. P.; Richardson, D. R. *J. Am. Chem. Soc.* **1975**, *97*, 7194.
(7) Mayer, L. A.; Brusted, R. C. *J. Coord. Chem.* **1973**, *3*, 85.
(8) Grenthe, I. *J. Am. Chem. Soc.* **1961**, *83*, 360.
(9) Donato, H.; Martin, R. B. *J. Am. Chem. Soc.* **1972**, *94*, 4129.
(10) Madaras, J. S.; Brittain, H. G. *Inorg. Chem.* **1980**, *19*, 3841.
(11) Madaras, J. S.; Brittain, H. G. *Inorg. Chim. Acta* **1980**, *42*, 109.

0020-1669/82/1321-2955$01.25/0